Journal of Molecular Structure 1312 (2024) 138679

Contents lists available at ScienceDirect

Journal of Molecular Structure

journal homepage: www.elsevier.com/locate/molstr

Positive cooperativity in binding: Spectroscopic characterization and dissociation energy of the anisole···$(CH_4)_2$ complex

James Makuvaza [1], Damian L. Kokkin, John Loman [2], Scott A. Reid [*]

Department of Chemistry, Marquette University, Milwaukee, WI 53233, United States

ARTICLE INFO

Keywords:
Noncovalent interactions
Cooperativity
Dispersion forcesm
Binding energies
Ion imaging

ABSTRACT

We have previously reported on the spectroscopy and binding energy of the anisole···methane complex, which exhibits a dual mode of binding that involves both C—H/O and C—H/π interactions. In this work, we seek to examine cooperativity in binding through a study of the isolated anisole-$(methane)_2$ complex, using a combination of experiments that include mass-selected two-color resonant two-photon ionization spectroscopy (2CR2PI), two-color appearance potential (2CAP) measurements, and velocity mapped ion imaging (VMI) augmented with a complementary theoretical characterization. Using 2CAP and VMI, we derive the dissociation energies of the complex in ground (S_0), excited (S_1), and cation radical (D_0) states. The experimental values from the two methods are in excellent agreement and are compared with selected theoretical values calculated using DFT and *ab initio* methods. The data show that the dissociation energy increases by some 10 % for the second methane relative to the first, with this trend being consistent across all three electronic states, indicating a cooperative binding effect where the initial solvation turns on binding of a second methane onto the opposite face. This lies in contrast to the aniline-$(methane)_2$ complex, where recent studies have shown a negativity cooperativity, and these trends are examined.

Data show that the dissociation energy increases by some 10 % for the second methane relative to the first, indicating a cooperative binding effect where the initial solvation turns on binding of a second methane onto the opposite face.

- This lies in contrast to the aniline-$(methane)_2$ complex, where recent studies have shown a negativity cooperativity

1. Introduction

The detailed mechanisms of solvation continue to be actively explored through the study of isolated molecular clusters, [1–6] yielding insights into the strength and mechanisms of hydrogen bonding, [7] halogen bonding and other sigma-hole type interactions, [8–10] π-π interactions, [3] C—H-π interactions, [11–19] and C—H-O interactions, [20–22] among others. Given their status as efficient chromophores amenable to detection via fluorescence and resonant ionization methods, model systems often consist of complexes of an aromatic moiety bound to different small polyatomic molecules. [2,23–27] Size-selected clusters can be readily prepared and interrogated through use of electronic and/or infrared spectroscopy combined with jet-cooled supersonic expansions (molecular beams). [6,28–32] The advent of velocity mapped ion imaging (VMI) has provided another tool for investigating the dissociation (binding) energies of clusters. [33–44]

Following initial solvation of the chromophore with a single solvent molecule, subsequent solvation will involve competition between self-interaction in the solvent and interaction with the solute, leading to differing solvation mechanisms. Studies of micro–solvation, exploring the role of competition between solute-solvent and solvent-solvent interactions, can be probed via the study of higher order complexes. For solvents with strong hydrogen bonding interactions, e.g. ammonia (dimer binding energy of 12.9 kJ/mol) [45] or water (dimer binding energy of 20.9 kJ/mol), [46] the solvent-solvent interaction may dominate. For example, studies of $PhCl\cdots(NH_3)_n$ (n = 1–3) complexes show that upon ionization, the $PhCl\cdots NH_3$ dimer (i.e., n = 1) cation radical reacts via two distinct pathways: 1) Cl atom loss, to give protonated aniline, and 2) HCl loss, to give the aniline cation radical. [47]

* Corresponding author.
E-mail address: scott.reid@marquette.edu (S.A. Reid).
[1] Present address.
[2] Present address.

https://doi.org/10.1016/j.molstruc.2024.138679
Received 28 March 2024; Received in revised form 15 May 2024; Accepted 18 May 2024
Available online 19 May 2024
0022-2860/© 2024 Elsevier B.V. All rights are reserved, including those for text and data mining, AI training, and similar technologies.

These reactive pathways are blocked in complexes with $n = 2$ and 3, presumably due to the larger self-interaction among the ammonia moieties.

The role of cooperativity in the dissociation energies of model complexes and clusters is an active research area. Representative studies include the examination of interplay between hydrogen bonding, anion-π and lone pair-π interactions in anion recognition, [48] the cooperativity of hydrogen and halogen bonding interactions, [49] competition between weak hydrogen bonds, [50] and the strengthening effect of halogen, chalcogen, and pnictogen bonding on the halogen-π interaction. [51] Experimental investigation of such effects in weakly bound complexes is challenging, yet significant progress has been made in the study of three body effects between aromatics and rare gases. For example, Hobza and coworkers determined the dissociation energies of benzene-Ar and benzene-Ar_2 clusters to be 649.2 cm^{-1} and 1324.7 cm^{-1} respectively, [52] indicating a positive cooperativity with increase in dissociation energy (i.e., binding) for the second Ar (+4 %). In a related study, Lawrence and Bellm investigated the dissociation energy for the loss of an Ar atom from the *p*-difluorobenzene-Ar_2 complex (339 cm^{-1}). [53] Using a previously derived value for the dissociation of the *p*-difluorobenzene-Ar complex (337 cm^{-1}), [35] they found that the two dissociation energies were consistent within experimental uncertainty, as the presence of the first Ar atom affected the dissociation energy of the second by less than ~ 2 %. Solvation of anisole with Ar atoms (n = 1–3) has been studied by Mazzoni et al., using a combination of quantum chemical calculations and high resolution resonant two-photon techniques. [54] The global minimum structure of the An···$(Ar)_2$ system found the Ar atoms sitting on opposite faces of the aromatic chromophore, and the addition of a third Ar had no distinct minimum. [55,56]

Complexes of two methane molecules with benzene, toluene, and aniline have previously been studied using Resonant 2-photon Ionization (R2PI) spectroscopy by Bernstein and co-workers. [57–61] Two distinct structures were considered, where the methane molecules were positioned on the same side or opposite sides of the aromatic ring. These early studies demonstrated a strong dependence of spectral shift of the origin band on cluster geometry. Taking benzene-methane as an example, the 1:2 cluster showed two distinct geometries which had different spectral shifts. [58] A conformer with the methane moieties on opposite sides of the ring gave a spectral shift in the origin band with respect to that of bare chromophore that was approximately additive; i.e., roughly *twice* that of the 1:1 complex. A second conformer, with the methane molecules on the same side of the aromatic ring, gave a non-additive spectral shift similar to that observed for the 1:1 cluster. In all cases the observed shifts of the complex bands were to the *red* (i.e., lower energy) of the bare chromophore.

Two distinct isomers were also found for the toluene-$(CH_4)_2$ complex. [59] Here, the isomer with both methane moieties on the same side exhibited an electronic origin that was shifted to the *blue* (i.e., higher energy) of the 1:1 complex, which was found roughly 43 cm^{-1} to the red of the toluene monomer origin. In contrast, the isomer where the methane moieties were found on opposite sides of the chromophore led to a larger red shift, again additive in being roughly twice that found for the 1:1 complex. These spectral shifts inherently reflect the relative difference in binding energy in the excited (S_1) and ground (S_0) states, and complexes of aromatics which involve the π system tend to be more strongly bound in the S_1 state and thus exhibit a spectral red-shift (vide infra). Thus, the origin position of the 1:2 "same side" isomer is consistent with disruption of the C—H/π interaction of the first methane by binding of the second. In contrast, the binding of a second methane on opposite face of the π-system leads to no such disruption and a larger red-shift from the monomer origin.

We recently examined cooperativity in the binding of aniline to methane through experimental and theoretical studies. [62] Derived dissociation energies of the 1:1 complex were measured in ground (S_0), excited (S_1), and cation radical (D_0) states, and the experimental results were in excellent agreement with theory. For the 1:2 complex, calculations predicted above that the most stable conformer consisted of methane moieties bound on opposite faces of the ring. Here a negative cooperativity was observed, where the dissociation energy for loss of a single methane from the 1:2 complex was smaller than that found for the 1:1 complex, a trend reproduced by theory.

Considering what is known for prior studies of the complexes of aromatics with methane, we thus expect for the anisole-$(CH_4)_2$ complex different possible structures where the two methane molecules are found on opposite sides of the aromatic ring or on the same side. However, anisole possesses two sites that can act as proton acceptors, the electron lone pair on oxygen and its aromatic π electron system, and therefore is a model system where C—H/π and C—H/O interactions occur in concert. In the present article, we examine cooperativity in the binding of methane to anisole by examining the spectroscopy and binding energy of the anisole-$(CH_4)_2$ complex. The experimental methods included mass-selected two-color R2PI spectroscopy (2CR2PI), two-color appearance potential (2CAP) measurements, and velocity mapped ion imaging (VMI). This study builds upon our prior study of the 1:1 complex, where, using 2CAP and VMI, we independently derived the dissociation energies of the complex in ground (S_0), excited (S_1), and cation radical (D_0) states, and found excellent agreement between the methods. The experimentally derived binding energies were compared with selected theoretical predictions from benchmarked DFT and *ab initio* methods, and the optimized ground state cluster geometry, in which methane sits above the ring and interacts with anisole via both C—H/π and C—H/O interactions, was consistent with experimental observations. The dual nature of the interaction was revealed by a larger ground state binding energy compared to the benzene-methane complex, where only C—H/π interactions are operative. Thus, solvation of anisole with a single methane occurs above the methoxy substituted ring carbon through the additive binding of both C—H/π and C—H/O interactions. [63]

1.1. Experimental and theoretical methods

Anisole···$(CH_4)_2$ clusters were prepared via the same method as previously used to produce anisole···methane clusters, by passing a premix of methane (10 %) in Ar carrier gas, at a backing pressure of 80 psi, through a bubbler containing liquid anisole (Sigma Aldrich, 99 % purity) held in a refrigerated bath maintained at –5 °C. This gas mixture was expanded into the source chamber of a R2PI time-of-flight (TOF) mass spectrometer via the 0.8 mm diameter orifice of a pulsed nozzle (General Valve series 9), and passing into the extraction region of the TOF through a 1.5 mm diameter conical nickel skimmer (Beam Dynamics). Resonant excitation was achieved using the frequency doubled output of a Nd:YAG pumped dye laser (Lambda-Physik Scanmate 2E pumped by the third harmonic of a Quantel Q-Smart 850 Nd:YAG laser), with ionization achieved using the tunable frequency doubled output of a second Nd:YAG pumped dye laser (Sirah Cobra-Stretch pumped by the second harmonic of a Spectra-Physics INDI Nd:YAG laser). Excitation and ionization lasers were overlapped spatially and temporally and counter-propagated through the TOF spectrometer. The counter-propagating lasers were loosely focused into the extraction region via 1.0 m (pump) or 2.0 m (probe) plano-convex focusing lenses and intersected perpendicularly with the supersonic molecular beam. In two-color experiments, the energy of the excitation laser was attenuated using a polarizer such that no one–color signal was observed.

Ionization yield spectra were then determined by setting the pump laser (λ_1) on resonance and scanning the frequency of the second laser (λ_2) through the ionization threshold, monitoring the anisole···(-methane)$_2$ mass channel. To determine binding energies, we used two-color appearance potential (2CAP) measurements, where the pump laser was set on resonance (λ_1) for the 1:2 complex, and the second (ionization) laser (λ_2) was scanned while monitoring the anisole(methane) mass channel. Temporal control of the experiment was achieved by use of an 8-channel digital pulse/delay generator (Berkeley Nucleonics 565).

Velocity-mapped ion imaging experiments were carried out in a separate spectrometer which utilized the same molecular beam source and has been described previously. [62,63] The gas mixture was expanded into the differentially pumped source chamber and the molecular beam entered the ionization region by passing through a 1.5 mm diameter conical nickel skimmer (Beam Dynamics). The lasers crossed the molecular beam between the first (repeller) and second (extractor) electrodes, downstream of the skimmer orifice, with their respective voltages tuned precisely, to obtain velocity mapping conditions. To collect images only on the mass feature of interest, the rear MCP voltage was gated over the time of flight of the species of interest. Ion images were typically acquired over several thousand laser shots (18000 for a 30-minute integration), with the signal attenuated by reduction of laser power to observe only a few ions each laser shot. The resultant images were background subtracted utilizing images obtained with λ_2 set below the fragmentation threshold, and the inverse Abel transform of the images was calculated using the pBASEX algorithm in a LABVIEW coded program.

In our previous work, various levels of theory were benchmarked against the experimental binding energy for the anisole···CH_4 cluster. [63] From these calculations B3LYP-D3, M06–2X and MP2 levels of theory, [64–68] employing the 6–311++*g*(3pd,3df) basis set, were found to determine values for the binding energies in the ground and cationic radical states in good agreement with experiment. Hence calculations were carried out on the anisole···$(CH_4)_2$ system employing the similar levels of theory. All calculations were undertaken using the G09 Rev D suite of computational chemistry programs on the Marquette *Pere* cluster.

2. Results and discussion

As illustrated in Fig. 1, geometry optimizations at the MP2/ 6–311++*G* (3df,3pd) level found three minimum energy structures for the 1:2 complex, as verified by frequency calculations which showed no imaginary frequencies. The calculated global minimum energy structure was structure **A**, where the methane molecules sat on opposite faces of the aromatic chromophore. In contrast, two structures (**B, C**) were found with the methane moieties on the same side of the aromatic ring.

The mass selected 2CR2PI spectra of anisole and the anisole-methane 1:1 and 1:2 clusters are presented in Fig. 2. The origin band of the 1:2 cluster is shown to be red shifted by 129 cm^{-1} with respect to the monomer origin, which is twice that of the anisole-methane 1:1 complex (64 cm^{-1}). This roughly additive spectroscopic shift is consistent with related studies of methane complexes with benzene and toluene, [58,59] and thus suggests that the two methane molecules occupy equivalent positions on opposite faces of the ring, consistent with the calculated global minimum energy structure shown in Fig. 1. Spectroscopic features close in frequency to the origin of the 1:1 cluster have been observed for both benzene···$(CH_4)_2$ and toluene···$(CH_4)_2$ and were assigned to conformers in which both methane moieties reside on the

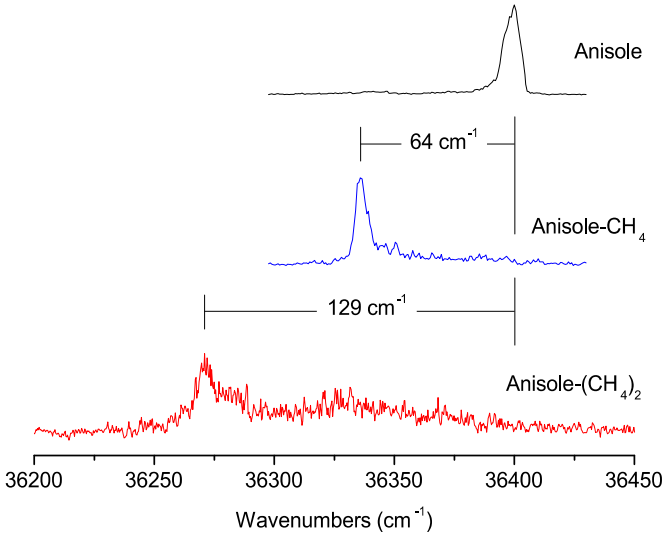

Fig. 2. R2PI spectra of anisole and the 1:1 and 1:2 complexes of anisole with methane.

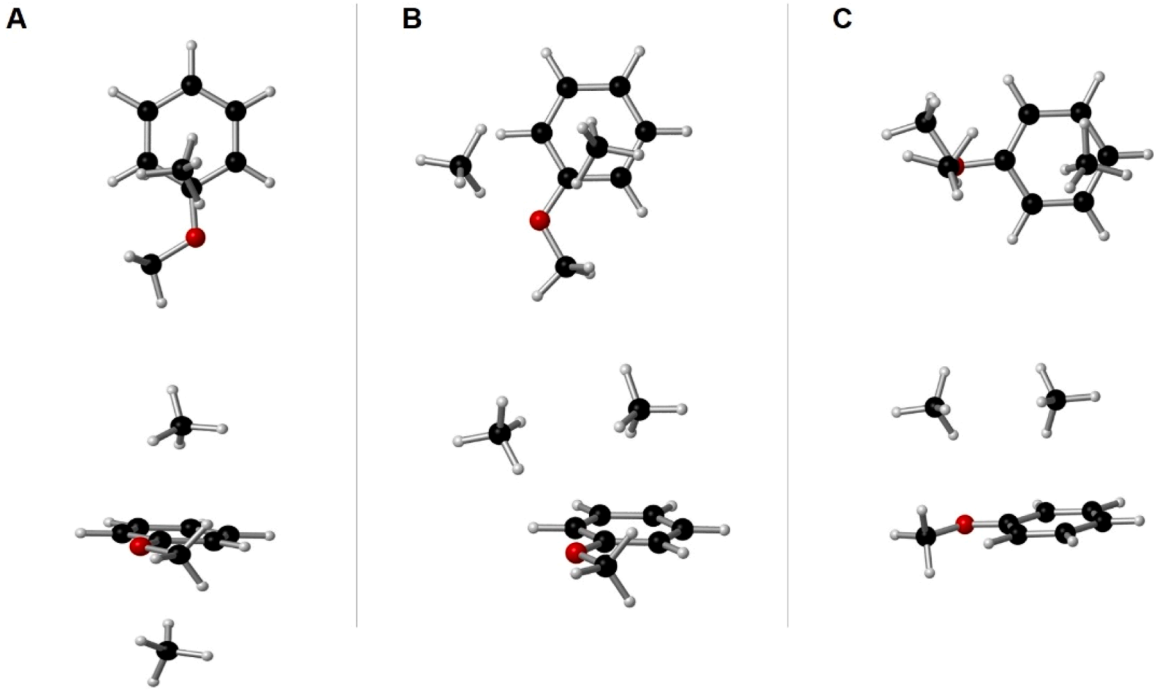

Fig. 1. Comparison of the ground state optimized structures of the anisole-methane 1:2 cluster from lowest energy to (A to C) at the MP2/ 6–311++*G* (3df,3pd) level. *A* = isotropic π-type geometry, *B* = anisotropic σ-π-type geometry and C = anisotropic π-type geometry.

same side of the ring. We find a broad, weak feature lying ~ 68 cm^{-1} from the monomer origin in the 1:2 cluster spectrum, which is slightly red shifted from the 1:1 complex origin. This could represent the origin of a second conformer of the 1:2 complex, or simply low frequency vibrational structure of the more sTable 1:2 complex. As the intensity of this feature is very weak, it was not considered further.

The measured ion yield curve for the anisole-methane 1:2 complex is shown as an inset in Fig. 3, together with that for the 1:1 cluster. The onset of the ion yield curve for the 1:2 cluster is more gradual compared to that of the 1:1 cluster, yet a clear threshold is observed around 8.151 (5) eV. This value is shifted to lower energy from the previously determined IP values for the anisole monomer and anisole-methane 1:1 complex, respectively. [63] This result can be interpreted on the basis of an increased stabilization of the cationic charge in the ionized cluster.

Fig. 3 highlights the thermochemical cycle used to derive the complex binding energies in S_0, S_1 and D_0 states. Using two-color appearance potential (2CAP) measurements, the binding energy of the anisole-methane 1:2 complex in the D_0 state was measured by monitoring the production of the anisole-methane cation radical (i.e., anisole-$(CH_4)^{+\bullet}$) from the fragmentation of the anisole-methane 1:2 complex as the ionizing laser was scanned. The energetic onset marking the appearance potential of anisole-$(CH_4)^{+\bullet}$ represents the sum of the of the ground state binding energy and the ionization potential of the anisole-methane complex as illustrated in the left panel (A) of Fig. 4. The 2CAP spectrum of the anisole-methane 1:2 cluster, plotted in terms of dissociation energy in the ground state (S_0) using the derived anisole-methane 1:1 complex IP, is shown on the right side of Fig. 4. An upper limit to the ground state (S_0) dissociation energy of 0.067(2) eV (or 6.5(2) kJ/mol) was obtained using a linear extrapolation. Application of the thermochemical cycle shown in Fig. 3 then returns dissociation energies of 0.075(2) and 0.103(2) eV for the S_1 and D_0 states, respectively, which represent upper limits to the true dissociation energies.

VMI experiments were also conducted to determine the binding energy of anisole-methane 1:2 cluster in the cation radical state (D_0) for comparison with results from the 2CAP measurements. The procedure used was similar to the one presented earlier for determination of the binding energies of the anisole-methane 1:1 complex, and involved measuring the kinetic energy of the anisole-$(CH_4)^{+\bullet}$ fragment following loss of a single methane from the ionized 1:2 complex. Fig. 5 displays VMI images obtained at different two-color energies of 8.226 eV (below dissociation threshold), 8.260 eV, and 8.283 eV. From analysis of the energetic cutoff in the transformed kinetic energy distribution, we derived an upper limit to the dissociation energy in the D_0 state of 0.102 (1) eV, or 9.8(1) kJ/mol. The corresponding binding energies for the S_1 and S_0 states from the VMI method were then obtained using the thermochemical cycle illustrated in Fig. 3.

The determined dissociation energies from the two experimental methods as propagated across all three electronic states are presented in Table 1, together with selected theoretical predictions. We first note that the 2CAP and VMI experimental results are in excellent agreement. Second, when compared with our earlier study of the 1:1 complex, these results show a 10 % increase in dissociation energy for the 1:2 complex across all three states (S_0, S_1, D_0). Thus, binding of the first methane molecule may have perturbed the electronic properties of the chromophore, leading to an increase in the binding interaction for the second methane. The difference in dissociation energy can be attributed to the presence of three body effects, [53] as observed for argon clusters of benzene and *p*-difluorobenzene. [53,69]

Table 1
Comparison of experimental and computed dissociation energies for the anisole-methane 1:2 complex. Experimental values list one standard deviation in parenthesis and all calculateddissociation energies were corrected for zero-point energy and basis set superposition error using the counterpoise method.

	Dissociation Energy (kJ/mol)		
Method	**S_0**	**S_1**	**D_0**
Experiment (2CAP)	6.5(3)	7.2(3)	9.9(4)
Experiment (VMI)	6.4(2)	7.1(2)	9.8(2)
PBE1-D3/aug-cc-pVTZ	6.4	…	9.9
PBE1-D3/6–311++*G*(3df,3pd)	6.0	…	9.6
M06–2X-D3/aug-cc-pVTZ	5.8	…	10.2
M06–2X-D3/6–311++*G*(3df,3pd)	5.7	…	10.8
B3LYP-D3/6–311++*G*(3df,3pd)	4.9	…	9.1
CAMB3LYP-D3/6–311++*G*(3df,3pd)	4.8	…	8.9
MP2/6–311++*G*(3df,3pd)	5.9	…	…

Turning to theoretical studies, representative structures of the anisole-methane 1:2 complex were presented earlier in Fig. 1. Calculations at the MP2/6–311++*G*(3dp,3df) level of theory show three structures corresponding to minima on the potential energy surface – two out of plane π-type geometries and one σ-type - π-type structure. Structure **A** in Fig. 1, which is the global minimum, has two methane molecules occupying equivalent positions above and below the plane of the anisole ring (isotropic cluster), while structures **B** and **C** have both methane molecules on the same side of the ring (anisotropic cluster). The global minimum energy structure is consistent with the additive red–shift in the excitation spectrum of the anisole-methane 1:2 complex, which is twice that observed for the 1:1 complex. Notably, the dual (i.e., C—H/O and C—H/π) mode of interaction is also evidenced in binding of the second methane. Prior studies of 1:2 complexes of benzene and toluene with methane have found the same type of geometries.[55,56] Our previous study of the anisole-methane 1:1 complex showed that, in addition to MP2, dispersion corrected DFT methods well reproduced the experimental results. We thus carried out complete geometry optimizations using the various DFT methods shown in Table 1, and in all cases the predicted global minimum energy structure was consistent with that shown in Fig. 1**A**. The calculated dissociation energies of the anisole-methane 1:2 complex in the ground (S_0) and cation radical (D_0) states are provided in Table 1. Noticeably, the B3LYP-D3 and CAMB3LYP-D3 methods underestimate the dissociation energies, particularly in the ground state. However, M06(2X) with both an aug-cc-pVTZ and 6–311++*g*(3dp,3df) basis set well reproduced the ground and excited state dissociation energies. We also found that the PBE1-D3 method showed good agreement with experimental dissociation energies and provided the best performance in both the neutral and cation radical states when matched with an aug-cc-pVTZ basis set.

As a further check on the optimized structures, calculations were carried out with tight optimization criteria in G16 using MP2 in combination with the 6–311++*g*(3df,3pd) basis set and the default ultrafine grid. No discernable difference were obtained in the calculated minimum energy structure and energetics. The calculated binding energy of 5.9 kJ/mol (corrected for ZPE and BSSE) is in excellent agreement with the experimental findings for the ground state (Table 1).

To gain more insights in the trend observed in dissociation energies of the 1:2 complex across the three electronic states, we carried out a Mulliken population analysis on the optimized structures of anisole, anisole-methane 1:1 and 1:2 complexes at the PBE1/aug-cc-pVTZ level of theory (Fig. 6). Charges on atoms were different across the monomer, 1:1 and 1:2 complexes and the dipole moment of the 1:2 complex was reduced (1.1693 D) relative to that of the 1:1 (1.2344 D) and monomer (1.2841 D). The low dipole moment is indicative of electron density being drawn from the methoxy group to the aromatic ring.

Finally, we compare the results from this study to our prior study of the aniline-$(CH_4)_2$ complex, which demonstrated a negative binding cooperativity. It is worth noting that the ground state (S_0) dissociation energy of the anisole-$(CH_4)_2$ complex is roughly 14 % higher than that of the corresponding aniline complex, which may reflect the non-planarity of the amino group in the ground state. In the cation radical state (D_0), the increase in dissociation energy is 25 %. In contrast, for the 1:1 complexes the anisole complex is *less strongly bound* in the ground state, by some 14 %, and more strongly bound in the cation radical state, by some 15 %. This further illustrates the positive cooperativity in the anisole-methane system.

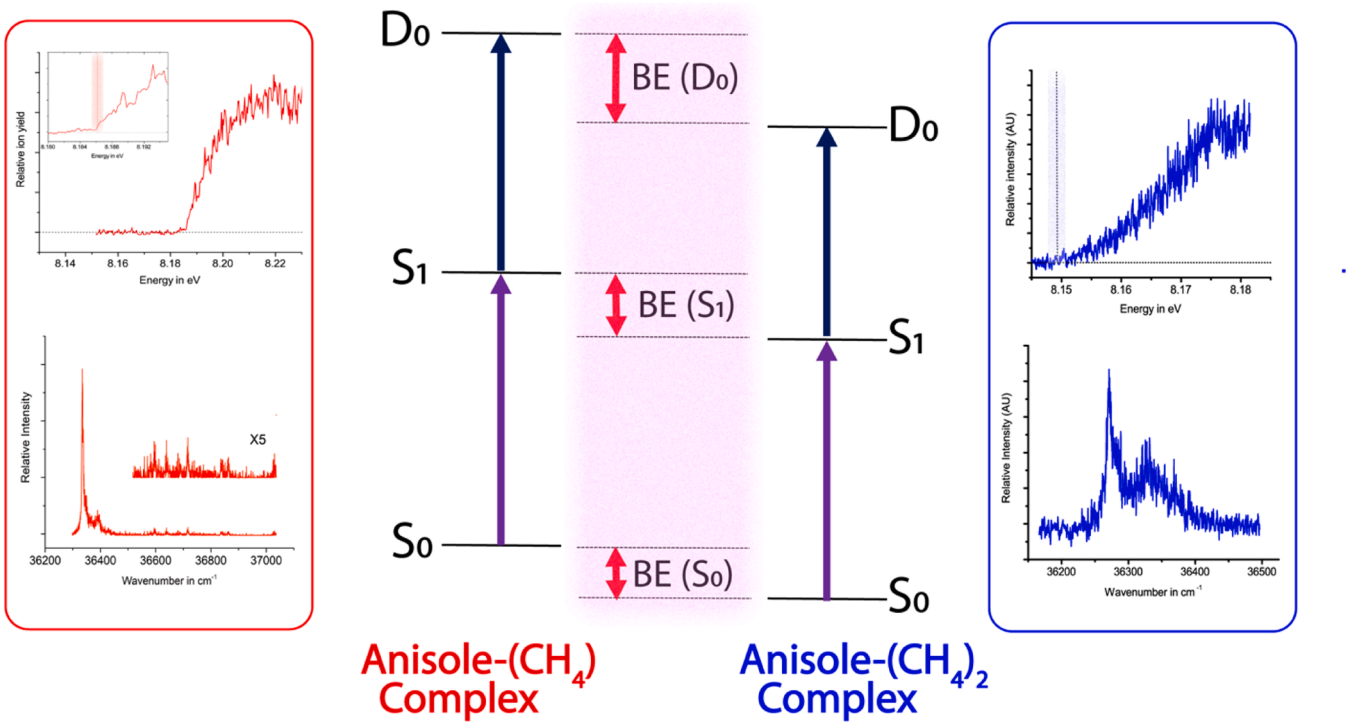

Fig. 3. A snapshot of spectroscopic data obtained for the 1:1 and 1:2 anisole-methane complexes, together with an energy ladder diagram. For each species, electronic spectra (S_0-S_1) were obtained in 2CR2PI experiments as described in the text (lower figure in each panel). Ion yield spectra were then obtained in 2CR2PI measurements using a tunable second photon, to determine the ionization thresholds (upper figure in each panel).

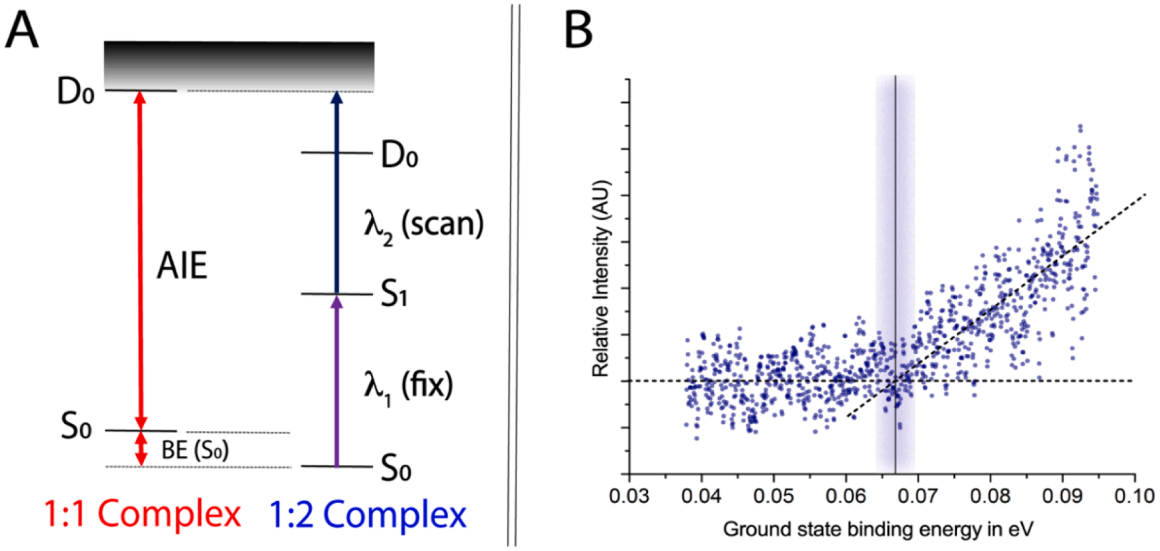

Fig. 4. A: Illustration of the 2CAP method as used to determine the dissociation energy of the 1:2 complex. Here the reference system is the 1:1 complex. B. 2CAP measurements for the anisole-methane 1:2 complex. The x-axis is scaled to reflect the ground state binding energy of the complex with respect to loss of a single methane.

3. Conclusions

As a means of probing cooperativity in C—H/O and C—H/π interactions, we have reported characterization of the spectroscopy and dissociation energies of anisole-methane 1:2 complex in ground (S_0), excited (S_1) and cation radical (D_0) states using R2PI and VMI techniques. The global minimum energy structure predicted by MP2 and dispersion corrected DFT methods shows a dual mode of interaction (C—H/O vs C—H/π) on opposite faces of the aromatic ring, which is consistent with the observed additive spectral red-shift of the electronic origin, which is roughly twice that observed for the 1:1 complex. Dissociation energy data for the anisole-methane 1:2 complex showed an increase of some 10 % for the second methane relative to the first, which was consistent across all three states, and indicative of positive cooperative in binding. The degree of cooperativity is further evidenced by comparison with the related aniline complex. Experimental dissociation energies were in good agreement with theoretical methods, with the PBE1-D3 method providing the most accurate description across the S_0 and D_0 states.

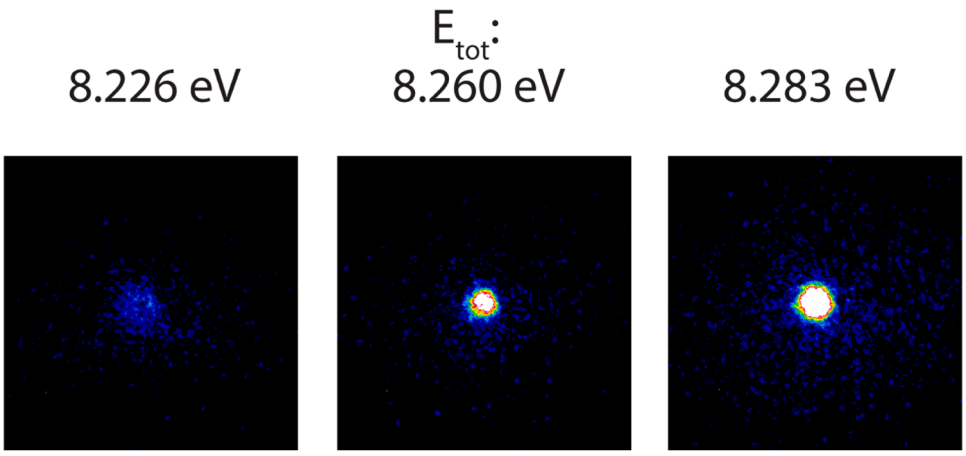

Fig. 5. Velocity mapped ion images of the 1:1 anisole-methane cation radical produced from dissociative ionization of the 1:2 anisole methane complex using two-color sequential ionization. In the panel at left, the total energy is below the fragmentation threshold.

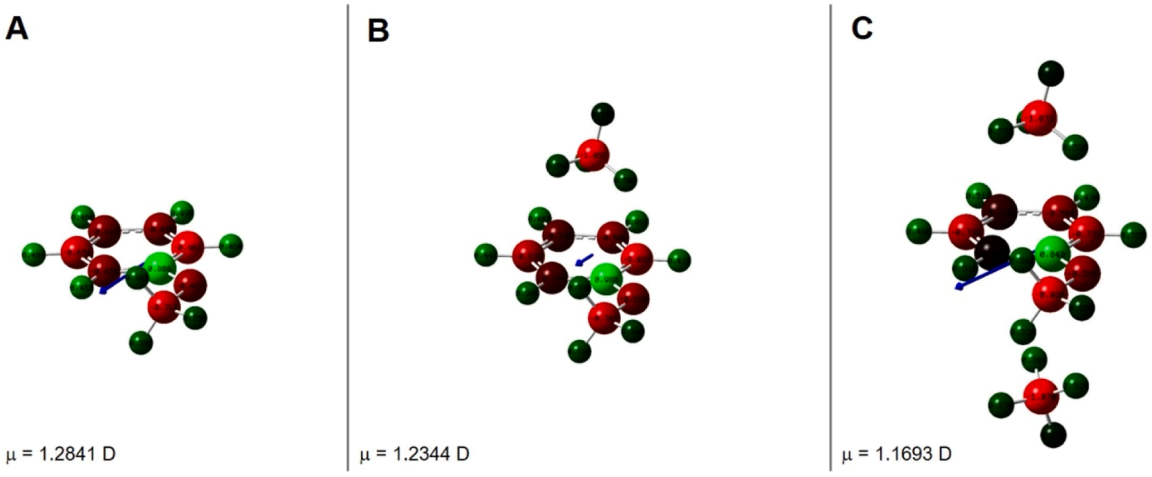

Fig. 6. Predicted atomic charges from Mulliken population analysis. *A* = anisole, *B* = anisole-methane 1:1 complex and C = anisole-methane 1:2 complex at the PBE1-D3/aug-cc-pVTZ level.

CRediT authorship contribution statement

James Makuvaza: Formal analysis, Data curation. **Damian L. Kokkin:** Writing – original draft, Supervision, Formal analysis, Data curation. **John Loman:** Data curation. **Scott A. Reid:** Writing – review & editing, Project administration, Methodology, Funding acquisition, Conceptualization.

Declaration of competing interest

The authors declare the following financial interests/personal relationships which may be considered as potential competing interests:

Scott Reid reports financial support was provided by National Science Foundation. If there are other authors, they declare that they have no known competing financial interests or personal relationships that could have appeared to influence the work reported in this paper.

Data availability

Data will be made available on request.

Acknowledgements

We acknowledge financial support from the National Science Foundation (CHE- 2102548). Calculations were performed on the NSF supported high-performance computing clusters Père and Raj (MRI-1828649) at Marquette University. JM gratefully acknowledges receipt of an O'Brien Graduate Fellowship.

References

[1] H.J. Schneider, Non-covalent interactions, J. Phys. Org. Chem. 10 (5) (1997), 253-253.
[2] L. Muzangwa, S. Nyambo, B. Uhler, S.A. Reid, On pi-stacking, C-H/pi, and halogen bonding interactions in halobenzene clusters: resonant two-photon ionization studies of chlorobenzene, J. Chem. Phys. 137 (18) (2012).
[3] K.S. Kim, P. Tarakeshwar, J.Y. Lee, Molecular clusters of π-systems:: Theoretical studies of structures, spectra, and origin of interaction energies, Chem. Rev. 100 (11) (2000) 4145–4185.
[4] S.R. Gadre, S.D. Yeole, N. Sahu, Quantum chemical investigations on molecular clusters, Chem. Rev. 114 (24) (2014) 12132–12173.
[5] H. Sun, R.O. Watts, U. Buck, The infrared-spectrum and structure of hydrogen-fluoride clusters and the liquid - semiclassical and classical-studies, J. Chem. Phys. 96 (3) (1992) 1810–1821.
[6] U. Buck, Structure and dynamics of size selected molecular clusters, Ber Bunsen Phys. Chem. 96 (9) (1992) 1275–1284.
[7] R.K. Castellano, Special issue: intramolecular hydrogen bonding, Molecules 19 (10) (2014) 15783–15785.

[8] P. Politzer, J.S. Murray, An overview of strengths and directionalities of noncovalent interactions: σ-holes and π-holes, Crystals 9 (3) (2019).
[9] P. Politzer, J.S. Murray, T. Clark, G. Resnati, The σ-hole revisited, Phys. Chem. Chem. Phys. 19 (48) (2017) 32166–32178.
[10] P. Politzer, J.S. Murray, σ-Hole Interactions: perspectives and Misconceptions, Crystals 7 (7) (2017).
[11] S. Re, S. Nagase, How is the CH/π interaction important for molecular recognition? Chem. Commun. (6) (2004) 658–659.
[12] M. Nishio, The CH/π hydrogen bond in chemistry. Conformation, supramolecules, optical resolution and interactions involving carbohydrates, Phys. Chem. Chem. Phys. 13 (31) (2011) 13873–13900.
[13] O. Takahashi, Y. Kohno, S. Iwasaki, K. Saito, M. Iwaoka, S. Tomoda, Y. Umezawa, S. Tsuboyama, M. Nishio, Hydrogen-bond-like nature of the CH/π interaction as evidenced by crystallographic database analyses and ab initio molecular orbital calculations, B Chem. Soc. Jpn. 74 (12) (2001) 2421–2430.
[14] A. Fujii, H. Hayashi, J.W. Park, T. Kazama, N. Mikami, S. Tsuzuki, Experimental and theoretical determination of the accurate CH/π interaction energies in benzene-alkane clusters: correlation between interaction energy and polarizability, Phys. Chem. Chem. Phys. 13 (31) (2011) 14131–14141.
[15] A. Fujii, H. Hayashi, S. Tsuzuki, Preference of the monodentate contact in the CH/π interaction between an alkyl group and a single phenyl ring: stable structures of benzene-ethane clusters, Chem. Phys. Lett. 537 (2012) 11–15.
[16] A. Fujii, K. Shibasaki, T. Kazama, R. Itaya, N. Mikami, S. Tsuzuki, Experimental and theoretical determination of the accurate interaction energies in benzene-halomethane:: the unique nature of the activated CH/π interaction of haloalkanes, Phys. Chem. Chem. Phys. 10 (19) (2008) 2836–2843.
[17] S. Morita, A. Fujii, N. Mikami, S. Tsuzuki, Origin of the attraction in aliphatic C-H/π interactions: infrared spectroscopic and theoretical characterization of gas-phase clusters of aromatics with methane, J. Phys. Chem. A 110 (36) (2006) 10583–10590.
[18] S. Tsuzuki, A. Fujii, Nature and physical origin of CH/π interaction:: significant difference from conventional hydrogen bonds, Phys. Chem. Chem. Phys. 10 (19) (2008) 2584–2594.
[19] S. Tsuzuki, K. Honda, A. Fujii, T. Uchimaru, M. Mikami, CH/π interactions in methane clusters with polycyclic aromatic hydrocarbons, Phys. Chem. Chem. Phys. 10 (19) (2008) 2860–2865.
[20] J. Czernek, J. Brus, V. Czerneková, L. Kobera, Quantifying the intrinsic strength of C-H●●● O intermolecular interactions, Molecules 28 (11) (2023).
[21] J. Dickerhoff, B. Appel, S. Müller, K. Weisz, Sugar-Edge interactions in a DNA-RNA G-quadruplex: evidence of sequential C-H●●●O hydrogen bonds contributing to RNA quadruplex folding, Angew Chem. Int. Edit. 55 (48) (2016) 15162–15165.
[22] M. Zierke, M. Smiesko, S. Rabbani, T. Aeschbacher, B. Cutting, F.H.T. Allain, M. Schubert, B. Ernst, Stabilization of branched oligosaccharides: lewis^xbenefits from a nonconventional C-H●●●O hydrogen bond, J. Am. Chem. Soc. 135 (36) (2013) 13464–13472.
[23] B. Reimann, K. Buchhold, H.D. Barth, B. Brutschy, P. Tarakeshwar, K.S. Kim, Anisole-(H2O)n (n=1-3) complexes: an experimental and theoretical investigation of the modulation of optimal structures, binding energies, and vibrational spectra in both the ground and first excited states, J. Chem. Phys. 117 (19) (2002) 8805–8822.
[24] G. Pietraperzia, M. Pasquini, N. Schiccheri, G. Piani, M. Becucci, E. Castellucci, M. Biczysko, J. Bloino, V. Barone, The gas phase anisole dimer: a combined high-resolution spectroscopy and computational study of a stacked molecular system, J. Phys. Chem. A 113 (52) (2009) 14343–14351.
[25] M. Becucci, F. Mazzoni, G. Pietraperzia, J. Rezác, D. Natchigallová, P. Hobza, Non-covalent interactions in anisole-(CO2) (n=1, 2) complexes, Phys. Chem. Chem. Phys. 19 (34) (2017) 22749–22758.
[26] F. Mazzoni, M. Pasquini, G. Pietraperzia, M. Becucci, Binding energy determination in a π-stacked aromatic cluster: the anisole dimer, Phys. Chem. Chem. Phys. 15 (27) (2013) 11268–11274.
[27] N. Schiccheri, M. Pasquini, G. Piani, G. Pietraperzia, M. Becucci, M. Biczysko, J. Bloino, V. Barone, Integrated experimental and computational spectroscopy study on π-stacking interaction: the anisole dimer, Phys. Chem. Chem. Phys. 12 (41) (2010) 13547–13554.
[28] J. Jortner, U. Even, A. Goldberg, I. Schek, T. Raz, R.D. Levine, Energetics and dynamics of molecular clusters, Surf. Rev. Lett. 3 (1) (1996) 263–280.
[29] R. Knochenmuss, R.K. Sinha, S. Leutwyler, Intermolecular dissociation energies of dispersively bound complexes of aromatics with noble gases and nitrogen, J. Chem. Phys. 148 (13) (2018).
[30] T. Stace, Chemical physics - cooling of molecular clusters, Nature 327 (6119) (1987) 186–187.
[31] D. Herschbach, Chemical physics: molecular clouds, clusters, and corrals, Rev. Mod. Phys. 71 (2) (1999) S411–S418.
[32] J.A. Frey, C. Holzer, W. Klopper, S. Leutwyler, Experimental and theoretical determination of dissociation energies of dispersion-dominated aromatic molecular complexes, Chem. Rev. 116 (9) (2016) 5614–5641.
[33] A.T.J.B. Eppink, D.H. Parker, Velocity map imaging of ions and electrons using electrostatic lenses: application in photoelectron and photofragment ion imaging of molecular oxygen, Rev. Sci. Instrum. 68 (9) (1997) 3477–3484.
[34] D.H. Parker, A.T.J.B. Eppink, Photoelectron and photofragment velocity map imaging of state-selected molecular oxygen dissociation/ionization dynamics, J. Chem. Phys. 107 (7) (1997) 2357–2362.
[35] S.M. Bellm, R.J. Moulds, M.P. van Leeuwen, W.D. Lawrance, A velocity map ion imaging study of difluorobenzene-water complexes: binding energies and recoil distributions, J. Chem. Phys. 128 (11) (2008).
[36] R.K. Sampson, W.D. Lawrance, The dissociation energy of the benzene-argon Van der Waals complex determined by velocity map imaging, Aust. J. Chem. 56 (4) (2003) 275–277.
[37] S.M. Bellm, J.R. Gascooke, W.D. Lawrance, The dissociation energy of van der Waals complexes determined by velocity map imaging: values for S0 and S1 p-difluorobenzene-Ar and D0 (p-difluorobenzene-Ar)+, Chem. Phys. Lett. 330 (1–2) (2000) 103–109.
[38] A.K. Mollner, B.E. Casterline, L.C. Ch'ng, H. Reisler, Imaging the state-specific vibrational predissociation of the ammonia-water hydrogen-bonded dimer, J. Phys. Chem. A 113 (38) (2009) 10174–10183.
[39] H. Reisler, Photofragment spectroscopy and predissociation dynamics of weakly bound molecules, Annu. Rev. Phys. Chem. 60 (2009) 39–59.
[40] J.S. Mancini, A.K. Samanta, J.M. Bowman, H. Reisler, Experiment and theory elucidate the multichannel predissociation dynamics of the HCl trimer: breaking up is hard to do, J. Phys. Chem. A 118 (37) (2014) 8402–8410.
[41] A.K. Samanta, G. Czakó, Y.M. Wang, J.S. Mancini, J.M. Bowman, H. Reisler, Experimental and theoretical investigations of energy transfer and hydrogen-bond breaking in small water and HCl clusters, Accounts Chem. Res. 47 (8) (2014) 2700–2709.
[42] A. Samanta, K. Zuraski, D. Kwasniewski, H. Reisler, Imaging bond breaking and vibrational energy transfer in hydrogen-bonded clusters, Abstr. Pap. Am. Chem. S (2016) 251.
[43] G.S. Li, J. Parr, I. Fedorov, H. Reisler, Imaging study of vibrational predissociation of the HCl-acetylene dimer: pair-correlated distributions, Phys. Chem. Chem. Phys. 8 (25) (2006) 2915–2924.
[44] J.A. Parr, G. Li, I. Fedorov, A.J. McCaffery, H. Reisler, Imaging the state-specific vibrational predissociation of the C2H2-NH3 hydrogen-bonded dimer, J. Phys. Chem. A 111 (31) (2007) 7589–7598.
[45] J.C. Greer, R. Ahlrichs, I.V. Hertel, Binding-Energies and Structures of Nh3 Clusters, Chem. Phys. 133 (2) (1989) 191–197.
[46] M.W. Feyereisen, D. Feller, D.A. Dixon, Hydrogen bond energy of the water dimer, J. Phys. Chem. Us 100 (8) (1996) 2993–2997.
[47] S.A. Reid, S. Nyambo, A. Kalume, B. Uhler, C. Karshenas, L. Muzangwa, Reactive pathways in the chlorobenzene-ammonia dimer cation radical: new insights from experiment and theory, J. Phys. Chem. A 117 (47) (2013) 12429–12437.
[48] M.E. Alberto, G. Mazzone, N. Russo, E. Sicilia, The mutual influence of non-covalent interactions in π-electron deficient cavities: the case of anion recognition by tetraoxacalix[2]arene[2]triazine, Chem. Commun. 46 (32) (2010) 5894–5896.
[49] S.J. Grabowski, Cooperativity of hydrogen and halogen bond interactions, Theor. Chem. Acc. 132 (4) (2013).
[50] H.L. Zhao, S.S. Tang, Q. Zhang, L. Du, Weak hydrogen bonding competition between O-H...π and O-H...Cl, RSC Adv. 7 (36) (2017) 22485–22491.
[51] M.D. Esrafili, P. Mousavian, The strengthening effect of a halogen, chalcogen or pnicogen bonding on halogen-π interaction: a comparative study, Mol. Phys. 116 (4) (2018) 526–535.
[52] P. Hobza, O. Bludsky, H.L. Selzle, E.W. Schlag, Ab initio calculations on the structure, vibrational frequencies, and valence excitation energies of the benzene center dot center dot center dot center dot Ar and benzene center dot center dot center dot Ar-2 cluster, Chem. Phys. Lett. 250 (3–4) (1996) 402–408.
[53] S.M. Bellm, W.D. Lawrance, The binding energy of Ar to p-difluorobenzene-Ar.: how large are three-body effects in p-difluorobenzene-Ar? Chem. Phys. Lett. 368 (5–6) (2003) 542–546.
[54] F. Mazzoni, M. Becucci, J. Rezác, D. Nachtigallová, F. Michels, P. Hobza, K. Müller-Dethlefs, Structure and energetics of the anisole-Arn (n=1, 2, 3) complexes: high-resolution resonant two-photon and threshold ionization experiments, and quantum chemical calculations, Phys. Chem. Chem. Phys. 17 (19) (2015) 12530–12537.
[55] M. Schmidt, M. Mons, J. Lecalve, Intermolecular vibronic spectroscopy of small vanderwaals clusters - phenol-(argon)2 and aniline-(argon)2 complexes, Z Phys. D Atom Mol. Cl 17 (2) (1990) 153–155.
[56] M. Takahashi, H. Ozeki, K. Kimura, Vibrational-Spectra of aniline-Ar-N Vanderwaals cations (N = 1 and 2) observed by 2-color threshold photoelectron [zero kinetic-energy (zeke)-photoelectron] spectroscopy, J. Chem. Phys. 96 (9) (1992) 6399–6406.
[57] M. Schauer, E.R. Bernstein, Calculations of the geometry and binding-energy of aromatic dimers - benzene, toluene, and toluene benzene, J. Chem. Phys. 82 (8) (1985) 3722–3727.
[58] M. Schauer, E.R. Bernstein, Molecular jet study of the solvation of benzene by methane, ethane, and propane, J. Chem. Phys. 82 (2) (1985) 726–735.
[59] M. Schauer, K.S. Law, E.R. Bernstein, Molecular jet study of the solvation of toluene by methane, ethane, and propane, J. Chem. Phys. 82 (2) (1985) 736–746.
[60] E.R. Bernstein, K. Law, M. Schauer, Molecular jet study of aniline helium Vanderwaals molecules and aniline radiationless relaxation in the 1b2 excited electronic state, J. Chem. Phys. 80 (1) (1984) 207–220.
[61] M. Schauer, K. Law, E.R. Bernstein, Supersonic molecular jet studies of toluene-helium and toluene-methane clusters, J. Chem. Phys. 81 (1) (1984) 49–56.
[62] J.T. Makuvaza, J.L. Loman, D.L. Kokkin, S.A. Reid, Probing cooperativity in C-HN and C-H pi interactions: dissociation energies of aniline(CH4)(n) (n=1, 2) van der Waals complexes from resonant ionization and velocity mapped ion imaging measurements, J. Chem. Phys. 153 (4) (2020).
[63] J.T. Makuvaza, D.L. Kokkin, J.L. Loman, S.A. Reid, C-H/pi and C-H-O interactions in concert: a study of the anisole-methane complex using resonant ionization and velocity mapped ion imaging, J. Phys. Chem. A 123 (13) (2019) 2874–2880.
[64] L. Goerigk, How Do DFT-DCP, DFT-NL, and DFT-D3 compare for the description of london-dispersion effects in conformers and general thermochemistry? J. Chem. Theory Comput. 10 (3) (2014) 968–980.

[65] D.A. Sirianni, A. Alenaizan, D.L. Cheney, C.D. Sherrill, Assessment of Density Functional Methods for Geometry Optimization of Bimolecular van der Waals Complexes, J. Chem. Theory Comput. 14 (6) (2018) 3004–3013.
[66] Y. Wang, P. Verma, X.S. Jin, D.G. Truhlar, X. He, Revised M06 density functional for main-group and transition-metal chemistry, Proc. Natl. Acad. Sci. USA 115 (41) (2018) 10257–10262.
[67] D. Quiñonero, A. Frontera, D. Escudero, P. Ballester, A. Costa, P.M. Deyà, MP2 Study of synergistic effects between X-H/π (X = C,N,O) and π-π interactions, Theor. Chem. Acc. 120 (4–6) (2008) 385–393.
[68] Y. Zhao, D.G. Truhlar, The M06 suite of density functionals for main group thermochemistry, thermochemical kinetics, noncovalent interactions, excited states, and transition elements: two new functionals and systematic testing of four M06-class functionals and 12 other functionals, Theor. Chem. Acc. 120 (1–3) (2008) 215–241.
[69] S.M. Bellm, W.D. Lawrance, The partitioning of energy amongst vibration, rotation, and translation during the dissociation of p-difluorobenzene-Ar neutral and cation complexes, J. Chem. Phys. 118 (6) (2003) 2581–2589.